Radiotherapy and Oncology 138 (2019) 52–58

Contents lists available at ScienceDirect

Radiotherapy and Oncology

journal homepage: www.thegreenjournal.com

Original Article

Inclusion of heart substructures in the optimization process of volumetric modulated arc therapy techniques may reduce the risk of heart disease in Hodgkin's lymphoma patients

Mario Levis [a,*], Andrea Riccardo Filippi [b], Christian Fiandra [a], Viola De Luca [a], Sara Bartoncini [a], Dwayne Vella [c], Riccardo Ragona [a], Umberto Ricardi [a]

[a] Department of Oncology, University of Torino; [b] Radiation Oncology Unit, Fondazione IRCCS Policlinico San Matteo, Pavia, Italy; [c] Sir Anthony Mamo Oncology Centre, Radiation Oncology, Msida, Malta

ARTICLE INFO

Article history:
Received 14 December 2018
Received in revised form 7 May 2019
Accepted 8 May 2019
Available online 27 May 2019

Keywords:
Hodgkin lymphoma
IMRT/VMAT
Radiotherapy
Heart toxicity
Cardiac risk
Second cancers

ABSTRACT

Background and purpose: Radiotherapy is an effective treatment for Hodgkin's lymphoma (HL), but increases the risk of long term complications as cardiac events and second cancers. This study aimed to reduce the risk of cardiovascular events through an optimization of the dose distribution on heart substructures in mediastinal HL patients with the adoption of different volumetric modulated arc therapy (VMAT) techniques, while maintaining the same risk of second cancer induction on lungs and breasts.

Materials and methods: Thirty patients (15 males and 15 females, 15 bulky lesions) treated between 2012 and 2017 at our institution were selected. Disease extent was mediastinum plus neck ($n = 10$), mediastinum plus unilateral axilla ($n = 10$) and mediastinum alone ($n = 10$). Lungs, breasts, whole heart and sub-structures (coronary arteries, valves and chambers) were contoured as organs at risk and included in the optimization process. A "first-generation" multi-arc butterfly VMAT (B-VMAT) planning solution was compared to a full-arc butterfly VMAT (FaB-VMAT) approach, consisting of a full arc plus a non-coplanar arc. Lifetime attributable risk (LAR) of second breast and lung cancer and relative risk (RR) of coronary artery disease (CAD) and chronic heart failure (CHF) were estimated.

Results: FaB-VMAT resulted in lower mean dose to whole heart (7.6 vs 6.9 Gy, $p = 0.003$), all coronary arteries (16.1 vs 13.5 Gy, $p < 0.001$), left ventricle (4.2 vs 3.4 Gy, $p = 0.007$) and in lower V_{20Gy} to the lungs (15% vs 14%, $p = 0.008$). A significant lower RR for CAD and CHF was observed for FaB-VMAT. The risk of second breast and lung cancer was comparable between the two solutions, with the exception of female patients with mediastinal bulky involvement, where B-VMAT resulted in lower mean dose (2.8 vs 3.5 Gy, $p = 0.03$) and V_{4Gy} (22% vs 16%, 0.04) to breasts, with a significant reduction in LAR ($p = 0.03$).

Conclusions: FaB-VMAT significantly decreased the RR for CAD and CHF compared to B-VMAT, with almost the same overall risk of lung and breast cancer induction. These results are influenced by the different anatomical presentations, supporting the need for an individualized approach.

The risk-adapted combination of brief chemotherapy followed by radiation therapy (RT), nowadays represents the therapeutic golden standard for early stage Hodgkin lymphoma (HL) [1]. Nonetheless, the role of radiation is still debated, with some concerns for late toxicity (second malignancies, heart disease). Current RT protocols combine limited radiation volumes (involved site or involved nodal radiotherapy, ISRT/INRT) with advanced planning and delivery techniques, such as intensity modulated RT (IMRT), tomotherapy and proton therapy. Different IMRT solutions have been implemented over the years, generally obtaining superior target coverage and better organs at risk (OARs) sparing, mainly heart and coronary arteries [2–4]. The heart sparing effect achievable by IMRT is usually counterbalanced by a more massive breast and lung volume receiving low or shallow radiation dose (below 5 Gy). Given this dose distribution, the appropriateness of IMRT in young HL patients has been questioned, assuming a potential increase in radiation-induced malignancies [5], being second cancers a leading cause of death among long-term survivors [6]. Second generation comparative planning studies [2,3] have further optimized heart sparing, adopting various technical solutions, and in most studies, the dose distribution on breasts and lungs did not translate in an increased risk of secondary cancer or a

* Corresponding author at: Department of Oncology, University of Torino, Via Genova3, 10126 Torino, Italy.
E-mail address: mario.levis@unito.it (M. Levis).

https://doi.org/10.1016/j.radonc.2019.05.009
0167-8140/

reduction in life expectancy estimated through different predictive models [7–11]. New epidemiological evidence also showed a very low incidence of radiation-induced second cancer in adults exposed to fractionated low-dose RT, with most of the tumors arising in the high-intermediate dose region [12]. The variable anatomic presentation of early-stage HL may significantly affect the risk of second cancer and heart disease of survivors on an individual basis, a factor that often steers the selection of the appropriate planning solution. For patients with supra-diaphragmatic HL the so-called "Butterfly" volumetric modulated arc therapy (B-VMAT) class solution [8,13], consisting of a multi-arc beam arrangement, was developed a few years ago. B-VMAT was primarily optimized on breasts and lungs and secondly on the whole heart. In the first series of anatomical presentations, this approach resulted superior to 3D conformal radiotherapy for heart sparing, with acceptable exposure of lungs and breasts when these structures were delineated and dedicated dose constraints applied. Afterward, heart toxicity further emerged as a critical point, given its linear correlation with mean heart dose [14–17]. Some studies have then investigated the dose–response relationship of single heart substructures [18,19], suggesting that full heart dose should not be anymore considered the best predictor for all types of radiation-related heart disease, recommending accurate contouring of all substructures (valves, coronary arteries, chambers). We partially modify the B-VMAT solution, to further improve the dosimetric profile and the associated risk of developing coronary artery disease (CAD) and chronic heart failure (CHF), while keeping a similar second cancer induction risk. The main aim of this study is thus to compare a new IMRT approach with our previous *golden standard*, represented by the B-VMAT solution, among a cohort of patients treated with ISRT for different anatomical presentations of mediastinal HL.

Material and methods

Patients

In this retrospective comparative analysis, 30 patients (15 males and 15 females) affected with mediastinal HL were included. All patients were treated between 2012 and 2017 with ABVD (doxorubicin, bleomycin, vinblastine, and dacarbazine) chemotherapy followed by ISRT. The population was divided into three homogeneous groups according to disease presentation at diagnosis, as shown in Fig. 1. Male and female patients were equally distributed in the three subgroups. Patients were selected in respect of the criteria mentioned above, provided the availability of complete contouring of all OARs. Twenty-one patients (70%) had a stage I-II, while the remaining 9 (30%) had a stage III-IV disease. Fifteen patients (50%) had a bulky disease at diagnosis (>10 cm on the maximum axis). Detailed patient characteristics are presented in Table 1.

Table 1
Patients' characteristics.

Characteristic	Number	%
Patients	30	100
Age (years)		
Range	15–48	
Median	25,5	
Sex		
Male	15	50%
Female	15	50%
Ann Arbor Stage		
I	2	7%
II	19	63%
III	4	13%
IV	5	17%
Bulky disease	15	50%
Involved Sites		
Mediastinum alone	10	33%
Mediastinum + axilla	10	33%
Mediastinum + neck	10	33%

Radiation therapy technique

The same two radiation oncologists performed the delineation of clinical target volumes (CTV) and OAR for all patients. CTV were delineated as involved sites. A 5-mm isotropic margin was added to the CTV to generate planning target volumes (PTV), considering the use of daily cone-beam computed tomography (CT) image guidance. Lungs, thyroid, breasts, and cardiovascular structures (whole heart; left main, left anterior descending, circumflex and right coronary arteries; left and right ventricles, left and right atria; aortic, pulmonic, mitral and tricuspid valves) were defined as OARs and delineated on axial planning CT scans, that were acquired without intravenous (IV) contrast media injection. No auto-segmentation tools were adopted for this procedure. Therefore, all heart structures were manually contoured based on a slice-by-slice delineation according to the atlas published by Feng et al. [20], which provided a detailed description of the heart anatomy. The adoption of such contouring guidelines for the heart structures allowed to compensate for the omission of IV contrast injection; indeed, Feng et al. [20] noticed no improvement of contour accuracy or dose reporting with IV contrast infusion when their atlas was applied properly. A specific expansion margin for coronary arteries was adopted as derived from a previous study that estimated the displacement of coronary arteries related to the heart motion by the use of ECG-gated CT scans. [21]. Briefly, the isotropic expansion margin, detected through the application of the McKenzie–van Herk formula for organs at risk, was: 5 mm for left anterior descending and right coronary arteries, 4 mm for circumflex and 3 mm for the left main trunk. Prescription dose was 30 Gy in 2-Gy daily fractions for all patients. All dose constraints for breasts and lungs were derived from previous studies

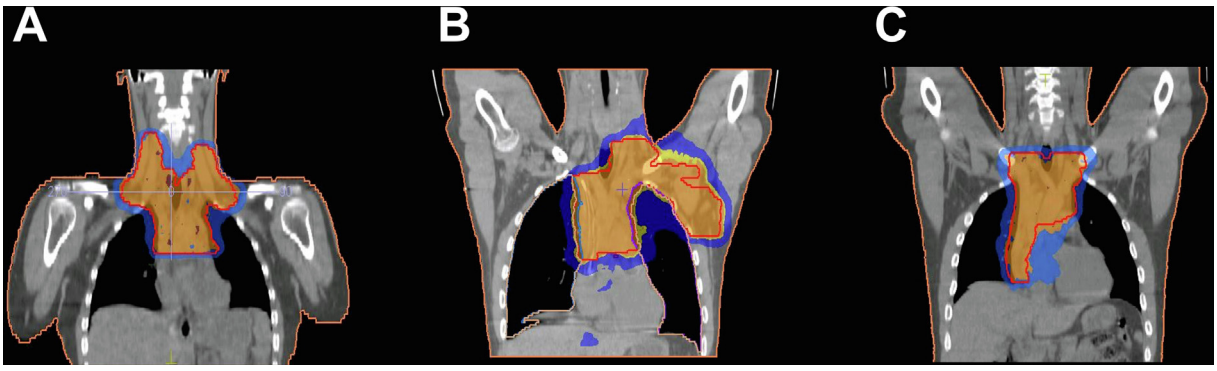

Fig. 1. Disease presentation of the 30 patients enrolled, equally distributed in the three groups: (A) mediastinum + neck; (B) mediastinum + axilla; (C) mediastinum alone.

[7,22]. Dose constraints were not set for heart substructures, given the different radiobiological features and lacking of precise limitations for the several tissues that cohabit in such a complex organ. In our opinion, a combined serial and parallel modeling might be reasonable, as the mean and maximum dose both appear significantly associated to ischemic disease [17,18,23]. Intending to control this process we used a biological optimization process on Elekta Monaco Treatment Planning System, version 5.0 (Crawley, UK), with two main cost-functions for organs at risk (serial and parallel complication models). The XVMC/VEF Monte Carlo algorithm with a 1.5% variance was used for all cases, and dose parameters for organs at risk were set according to an "As Low As Reasonably Achievable" optimization philosophy searching for the minimum dose to each involved OAR in terms of both mean and maximum doses.

Optimization was first directed to the coronary arteries, the left ventricle, and the aortic valve, as these structures have been considered highly relevant from a clinical point of view. Two multi-arc VMAT plans were then generated for each patient: the reference plan was a B-VMAT [13], consisting in 2 coplanar arcs of 60° (gantry starting angles of 150° and 330°) and 1 non-coplanar arc of 60° (gantry starting angle of 330° and couch angle of 90°). Beam arrangements were individually customized to provide tumor coverage while minimizing exposure to nearby critical organs. The guiding principle was avoiding lateral or near-lateral beams [3] to lower the dose bath on breasts and lungs (accepting a suboptimal conformality and PTV homogeneity). The investigational plan consisted of a complete coplanar arc of 360°, with the addition of the same trademark non-coplanar arc of 60° (gantry starting angle of 330° and couch angle of 90°) of the B-VMAT. For that reason, this new VMAT approach was called "*Full-arc Butterfly*" VMAT (FaB-VMAT). All patients were originally treated according to the B-VMAT plan and the FaB-VMAT plan was afterward simulated for this comparative study. Fig. 2 illustrates the two different class solutions.

Risk estimation and statistical analysis

For the second cancer risk estimation, we evaluated the lifetime attributable risk (LAR). Briefly, the process adopted to obtain this parameter is: (1) first of all, to evaluate the organ equivalent dose (OED) [24], as previously described in details [8]. OED can be calculated from the dose–volume histograms for each organ and represents the equivalent uniformly distributed dose (Gy), which causes the same radiation-induced cancer incidence. The dose–response relationship for each organ is derived by a combination between the low-dose component and an intermediate/high dose component. The formula we adopted from Schneider et al. [24] to evaluate OED is the following one:

$$\mathrm{OED} = 1/\mathrm{V_T}\sum_i \mathrm{V(D_i)RED(D_i)}$$

$$\text{With RED} = \exp^{-\alpha' D}/(\alpha R)\,(1 - 2R + 2R^2\exp^{\alpha' D} - (1-R)^2\exp(-\alpha' \mathrm{RD}/(1-R))$$

where $\alpha' = \alpha + \beta d$, α and β denoting the linear quadratic model parameters for the organ of interest and d dose per fraction. D is the total dose and R is the parameter of population/repair. $\alpha/\beta = 3$ Gy was used for calculation. For the risk of secondary tumor of breast and lung cancers the parameter of $\alpha = 0.067$; 0.042 Gy^{-1} and $R = 0.62$; 0.83 were used respectively. RED (risk equivalent dose) and OED were calculated from the relative dose–volume histograms. (2) From OED, we estimated the excess absolute risk (EAR) for a western population for each organ. (3) EAR was then translated to LAR, which is determined by the combination of age at exposure and life expectancy for each patient. Individual LAR values were calculated according to the equations previously published by Schneider et al. [25] and by Kellerer et al. [26]. For studies including subjects with limited follow-up time, Schneider et al. [25] suggested using a follow-up time interval instead of the life expectancy (estimated from the general population of the same age), and we used a 30-year time interval from radiation treatment. The model for the risk estimation of CAD was adopted from the publication by van Nimwegen et al. [17] for HL survivors. This risk model demonstrates a linear dose–response relationship between mean heart dose (MHD) and CAD risk, with an excess relative risk (ERR) for coronary events of 7.4% per Gy, and was first observed by Darby et al. [27] on breast cancer patients. We applied this dose–response relationship to the mean dose of the "overall coronary volume", defined as the sum of all the coronary tree. The choice was arbitrary, as no definitive data are available on dose–response relationship for coronary arteries. In our opinion, it was a realistic attempt to relate and to focus the risk of ischemic disease to the dose received by the endothelial heart tissue. For CHF estimation, we exploited the risk model recently published by van Nimwegen et al. [28], which found a linear dose–response relationship between mean left ventricular dose and CHF risk, with an ERR for clinical events of 9.0% per Gy. Based on the models mentioned above, relative risk (RR) was evaluated for both CAD and CHF. We then compared dosimetric parameters, mean values of LAR for second cancer risk and RR for CAD and CHF risk between B-VMAT and FaB-VMAT. The major parameters

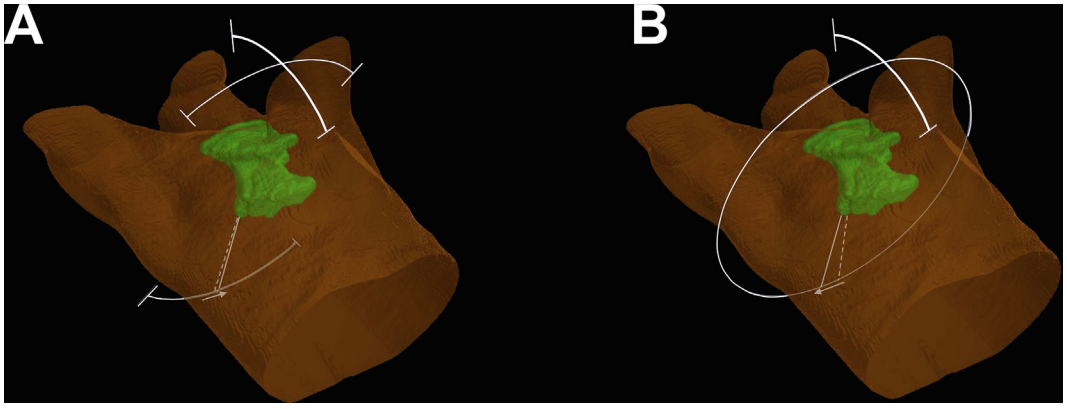

Fig. 2. Illustration of the two VMAT solution: (A) Butterfly VMAT (B-VMAT), consisting in 2 coplanar arcs of 60° (gantry starting angles of 150° and 330°) and 1 non-coplanar arc of 60° (gantry starting angle of 330° and couch angle of 90°); (B) Full-arc Butterfly VMAT (FaB-VMAT), consisting of a full coplanar arc of 360°, with the addition of the same non-coplanar arc of 60° (gantry starting angle of 330° and couch angle of 90°).

we measured were found to have a normal distribution, evaluated by means of the Shapiro–Francia test for normal distribution. Therefore, we used the Student paired t test, with a two-tailed significance level of 0.05, to perform the dosimetric comparison between B-VMAT and FaB-VMAT. Dose to 0.035 cc (D_{max}) and mean dose (D_{mean}) were reported for each OAR. We also assessed lung volume receiving 5 Gy ($V5_{Gy}$), 10 Gy ($V10_{Gy}$), 20 Gy ($V20_{Gy}$) and breast volume receiving 4 Gy ($V4_{Gy}$). All statistical analyses were performed using STATA version 13.1 statistical software (Stata Corporation, Texas, USA).

Results

D_{max}, D_{mean} and most significant volumetric parameters are reported for each structure and are summarized in Table 2.

A significant dosimetric difference between B-VMAT and FaB-VMAT was evident in favor of the latter one for lung V_{20Gy} (14% vs 15%, $p = 0.008$) and mean heart dose (6.9 Gy vs 7.6 Gy, $p = 0.003$), while mean breast dose (2.8 Gy vs 3.5 Gy, $p = 0.03$) and breast V_{4Gy} (16% vs 22%, $p = 0.04$) were slightly inferior with B-VMAT approach. Mean and maximum doses received by all the coronary arteries and by the left ventricle were significantly lower with FaB-VMAT, compared to B-VMAT. Fig. 3 shows the different dose distribution achievable with the two different VMAT approaches in a sample patient.

In the overall population, the dosimetric gain to the coronary arteries and the left ventricle translated in a lower relative risk (RR) for CAD (2.0 vs 2.2, $p < 0.01$) and CHF (1.3 vs 1.4, $p = 0.01$), respectively, with FaB-VMAT compared to B-VMAT. Moreover, FaB-VMAT provide a significant reduction in the risk in developing CAD to all subgroups of patients, regardless of disease presentation and gender, while conferred a significant lower risk of CHF to male patients ($p = 0.02$) and to those with bulky lesion ($p = 0.04$) or with mediastinal + axillary involvement ($p = 0.04$) and a marginal reduced risk in all other subgroups. On the other hand, LAR for breast and lung cancer did not differ between the two VMAT solutions. Relative risks (for CAD and CHF) and LAR (for lung and breast cancer), stratified for disease presentation and gender, are summarized in Table 3. With FaB-VMAT, LAR for breast cancer were

Table 2
Dose parameters to PTV and organs at risk for all 30 patients with B-VMAT and FaB-VMAT. Dosimetric parameters are presented as mean values ± SD.

Structure	Parameters	B-VMAT	FaB-VMAT	*p*-value
PTV	D_{mean} (Gy)	30.4 ± 1.9	30.4 ± 1.8	0.7
	D_{max} (Gy)	34.7 ± 2.1	34.6 ± 1.8	0.5
	$V95_{\%}$ (%)	94.3 ± 5.2	94.6 ± 2.9	0.8
	$V107_{\%}$ (%)	2.0 ± 1.0	2.0 ± 1.5	0.8
Lungs	D_{mean} (Gy)	7.5 ± 1.9	7.5 ± 1.7	0.9
	D_{max} (Gy)	33.4 ± 2.2	33.7 ± 1.9	0.4
	$V5_{Gy}$ (%)	39.8 ± 9.5	41.1 ± 7.4	0.2
	$V10_{Gy}$ (%)	27.9 ± 7.3	27.5 ± 7.1	0.4
	$V20_{Gy}$ (%)	15.4 ± 5.9	14.4 ± 5.4	0.008
Breasts	D_{mean} (Gy)	2.8 ± 3.0	3.5 ± 2.7	0.03
	D_{max} (Gy)	27.2 ± 9.5	27.7 ± 9.4	0.5
	$V4_{Gy}$ (%)	16.6 ± 16.1	22.2 ± 15.5	0.04
Heart	D_{mean} (Gy)	7.6 ± 5.1	6.9 ± 4.8	0.003
	D_{max} (Gy)	32.8 ± 3.6	32.5 ± 4.3	0.3
Coronary arteries				
1) Left main coronary	D_{mean} (Gy)	19.5 ± 7.7	15.9 ± 7.5	<0.001
	D_{max} (Gy)	25.8 ± 5.9	21.6 ± 7.4	<0.001
2) Left anterior descending	D_{mean} (Gy)	15.6 ± 9.0	13.2 ± 8.9	<0.001
	D_{max} (Gy)	26.2 ± 8.5	21.9 ± 10.6	<0.001
3) Left circumflex	D_{mean} (Gy)	14.0 ± 8.6	10.7 ± 7.8	<0.001
	D_{max} (Gy)	22.7 ± 7.9	17.9 ± 9.0	<0.001
4) Right coronary	D_{mean} (Gy)	17.0 ± 11.4	15.8 ± 11.6	0.005
	D_{max} (Gy)	23.1 ± 11.5	20.9 ± 12.6	0.006
5) Coronary sum (overall)	D_{mean} (Gy)	16.1 ± 9.3	13.5 ± 8.9	<0.001
	D_{max} (Gy)	29.6 ± 5.9	27.3 ± 8.2	0.002
Heart chambers				
1) Left atrium	D_{mean} (Gy)	13.1 ± 6.7	11.1 ± 6.6	0.4
	D_{max} (Gy)	29.2 ± 6.0	28.4 ± 7.1	0.8
2) Left ventricle	D_{mean} (Gy)	4.2 ± 4.7	3.4 ± 3.7	0.007
	D_{max} (Gy)	25.6 ± 9.8	21.9 ± 11.1	<0.001
3) Right atrium	D_{mean} (Gy)	12.6 ± 7.3	11.9 ± 7.7	0.09
	D_{max} (Gy)	30.8 ± 5.5	30.7 ± 5.3	0.9
4) Right ventricle	D_{mean} (Gy)	7.3 ± 6.2	7.0 ± 6.1	0.2
	D_{max} (Gy)	31.1 ± 5.7	30.2 ± 6.9	0.08
Heart valves				
1) Aortic valve	D_{mean} (Gy)	15.7 ± 9.0	13.2 ± 8.7	<0.001
	D_{max} (Gy)	23.3 ± 9.1	22.8 ± 10.0	0.4
2) Pulmonic valve	D_{mean} (Gy)	19.9 ± 7.7	18.7 ± 7.9	0.2
	D_{max} (Gy)	28.3 ± 6.4	26.7 ± 7.1	0.1
3) Mitral valve	D_{mean} (Gy)	9.0 ± 4.9	8.8 ± 7.5	0.9
	D_{max} (Gy)	19.9 ± 6.0	14.9 ± 10.4	0.2
4) Tricuspid valve	D_{mean} (Gy)	9.7 ± 8.5	9.4 ± 9.7	0.8
	D_{max} (Gy)	16.8 ± 10.8	15.0 ± 11.7	0.07

Abbreviations: B-VMAT = butterfly volumetric modulated arc therapy; FaB-VMAT = full-arc butterfly modulated arc therapy; D_{mean} = mean dose; D_{max} = maximum dose; Vx (%) = percentage of the target receiving X Gy.

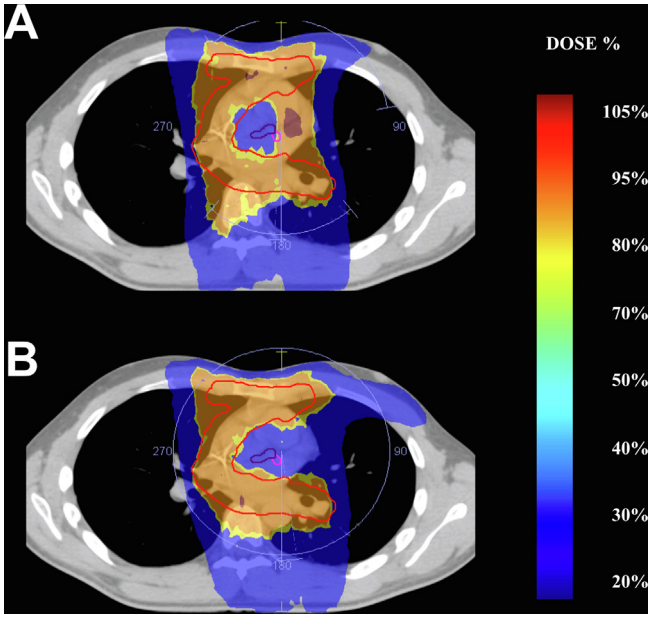

Fig. 3. Comparison between B-VMAT (A) and FaB-VMAT (B) in an enrolled patient (axial view). Notice the lower conformity of B-VMAT, generating hotspots in cardiac structures close to PTV (left main trunk in purple and circumflex in pink).

Table 3
Relative risks (for CAD and CHF) and LAR (for lung and breast cancer) in the overall population and stratified for disease presentation and gender.

Target	Mean value (±SD)		
	B-VMAT	FaB-VMAT	*p*-value
CAD (relative risk)			
-Overall population	2.2 ± 0.6	2.0 ± 0.6	**<0.01**
-Mediastinum + axilla	1.9 ± 0.5	1.7 ± 0.4	**<0.01**
-Mediastinum + neck	2.1 ± 0.7	1.9 ± 0.7	**<0.01**
-Mediastinum alone	2.6 ± 0.4	2.3 ± 0.3	**<0.01**
-Mediastinal Bulk (>10 cm)	2.6 ± 0.4	2.4 ± 0.4	**<0.01**
-Male gender	2.2 ± 0.6	2.1 ± 0.6	**<0.01**
-Female gender	2.1 ± 0.6	1.9 ± 0.6	**<0.01**
CHF (relative risk)			
-Overall population	1.4 ± 0.8	1.3 ± 0.6	**<0.01**
-Mediastinum + axilla	1.2 ± 0.2	1.2 ± 0.2	**0.04**
-Mediastinum + neck	1.5 ± 0.7	1.4 ± 0.5	0.08
-Mediastinum alone	1.4 ± 0.2	1.3 ± 0.2	0.1
-Mediastinal Bulk (>10 cm)	1.6 ± 0.5	1.5 ± 0.4	**0.04**
-Male gender	1.4 ± 0.2	1.3 ± 0.2	**0.02**
-Female gender	1.4 ± 0.5	1.3 ± 0.4	0.08
Second Lung Tumor (LAR)			
-Overall population	233.0 ± 63.9	245.0 ± 42.5	0.1
-Mediastinum + axilla	249.2 ± 58.6	251.1 ± 48.4	0.8
-Mediastinum + neck	218.5 ± 51.4	227.1 ± 48.0	0.2
-Mediastinum alone	231.6 ± 81.1	259.0 ± 23.2	0.3
-Mediastinal Bulk (>10 cm)	239.6 ± 67.7	257.2 ± 28.9	0.3
-Male gender	235.5 ± 40.1	234.5 ± 38.4	0.8
-Female gender	230.8 ± 82.7	257.2 ± 44.5	0.1
Second Breast Cancer (LAR)			
-Overall population	63.3 ± 51.1	77.0 ± 35.1	0.1
-Mediastinum + axilla	96.7 ± 66.5	87.9 ± 39.3	0.7
-Mediastinum + neck	30.4 ± 16.9	51.9 ± 32.7	0.08
-Mediastinum alone	62.7 ± 40.9	91.2 ± 22.5	0.07
-Mediastinal Bulk (>10 cm)	59.6 ± 37.4	88.5 ± 21.1	**0.03**

Abbreviations: SD = standard deviation; B-VMAT = butterfly volumetric modulated arc therapy; FaB-VMAT = full-arc butterfly modulated arc therapy.
CAD = coronary artery disease; CHF = chronic heart failure; LAR = life attributable risk.
Bold terms= statistically significant p values (< 0.05).

significantly higher (88.5 vs 59.6, $p = 0.03$) and breast V4 marginally higher (17% vs 27%, $p = 0.08$) in the subgroup of patients with bulky involvement at baseline. Moreover, with FaB-VMAT we observed a marginal increase in breast LAR also for patients with disease presentation in the mediastinum alone ($p = 0.07$ for each value) and in those with mediastinal + neck involvement ($p = 0.08$ for each value). When comparing LAR for breast cancer in female patients with axillary disease presentation, we found a similar risk between FaB-VMAT and B-VMAT. The risk of secondary lung cancer was almost identical for B-VMAT and FaB-VMAT across all subgroups.

Discussion

This study aimed to assess the ability of a new VMAT (FaB-VMAT) class solution to reduce the risk of CAD and CHF while maintaining a similar risk of developing second cancer in patients with mediastinal HL, also considering the potential impact of gender and different anatomical presentations. Our study has some relative strengths. First of all, we selected a cohort of patients with the most frequent anatomical presentation, including bulky and axillary involvement. Secondly, we treated all patients according to the ISRT concept, including only the lymphatic sites initially involved by macroscopic disease. Moreover, we outlined different heart structures and applied a specific margin for coronary arteries, compensating for motion. Finally, we adopted a biological optimization process working on multiple heart structures through an equivalent uniform dose based process, with dose constraints on breasts and lungs.

On these premises, the FaB-VMAT solution we tested did provide a higher beam conformation, compared to B-VMAT, in reason of the 360° arc, thus reducing hotspots to adjacent OARs. Our findings indicated that FaB-VMAT significantly decreases the maximum and mean dose received by the coronary arteries when compared to B-VMAT, and this dosimetric gain translated in a reduced risk of CAD. In the meantime, the risk of secondary breast and lung cancer was not statistically different between the two solutions in the overall population. After subgroup analysis, the impact of gender and anatomical presentation was not evident on dose distribution. The superiority of FaB-VMAT in sparing coronary arteries and in reducing the RR of CAD was then confirmed after stratification for these clinical factors. We noted a tendency toward an estimated slightly higher risk for breast cancer induction for FaB-VMAT for female patients with mediastinal involvement alone, but the limited sample size and the considerable heterogeneity in anatomical presentation hampers a valid comparison. A novelty of our study was the adaptation of the van Nimwegen model [17] to the mean dose of the "overall coronary volume" in replacement of the mean heart dose. The majority of studies have indeed shown a clear relationship between mean heart dose and all-cause heart toxicity [14,17,27,29], and there are uncertainties on the potential contribution of coronary arteries' dose–volume variables in risk estimation of heart disease. However, our results are consistent with a recent publication from the Princess Margaret Hospital Cancer Centre in Toronto [30], where firstly it has been shown that a risk model for ischemic disease including coronary artery variables is superior to a model purely based on the mean heart dose. On the other hand, the authors noticed that mean heart dose is still a sufficient parameter for the prediction of all-cause cardiac events. Unfortunately, van Nimwegen et al [17] did not evaluate coronary dose in their large cohort of long-term HL survivors. However, both a French [18] and a Swedish [31] group showed that the higher the dose, the greater was the damage to the coronary segments, suggesting the need for the integration of coronary dose parameters in the plan modeling. Likely, different heart substructures have different dose–risk relationships. Therefore plan optimization and adoption of dedicated dose constraints for each structure may be the best strategy to reduce

heart toxicity. However, despite an accurate contouring of all structures and the attempt to create dedicated risk-modeling, the estimation of cardiac events is still extremely complex, as many non RT-related factors such as the use of anthracyclines [29] and/or concomitant cardiovascular risk factors (hypertension, diabetes, dyslipidemia and obesity) [17,27] may have an impact. We also observed that the higher conformation provided by FaB-VMAT translates in a reduced risk of CHF in long-term survivors ($p = 0.01$), in reason of a better sparing of the left ventricle. This gain was maintained, at least marginally, across all groups of patients regardless of gender and disease presentation.

A limitation of our study is that the individual variations are substantial, and experiments comparing average doses or average risk estimates for different techniques may carry important limitations in describing what may happen in individual patients. Second cancer induction risk could also be dependent on factors such as inter-observer variability in target volumes and OAR delineation, margins around CTV and dose calculation uncertainty. Moreover, we may see a substantial difference in results when different radiobiological models are used. A systematic review of all published studies for secondary solid tumors after conventionally fractionated RT showed an overall tendency for a linear dose–response relationship, with the only exception of a downturn for thyroid cancer after 15–20 Gy, supporting the theoretical model we used [32]. Another limitation of our study is that we did not apply any form of breath motion control; this reflects our clinical practice at the time of study design (that is currently under review). The use of gating techniques, combined with daily image-guidance, has been shown to provide dosimetric benefits on heart and lungs when compared to free-breathing, and we may argue that when applying the same methods for breath control to different VMAT solutions, the full benefit of our full-arc approach would be maximized. A new research project is ongoing, introducing this further advancement in our workflow.

In conclusion, we here propose a FaB-VMAT solution that should be applicable to a large proportion of HL patients and that could be compared to other solutions to achieve the desired dose distribution on every single patient. Among a heterogeneous cohort of mediastinal HL patients, reflecting the most frequent clinical presentations, this novel FaB-VMAT solution significantly decreased the RR for CAD and CHF compared to B-VMAT, particularly in male patients, with similar breast and lung cancer risks in the overall population.

Funding source

None.

Declaration of Competing Interest

None.

References

[1] Eichenauer DA, Aleman BMP, André M, Federico M, Hutchings M, Illidge T, ESMO Guidelines Working Group. Hodgkin lymphoma: ESMO clinical practice guidelines for diagnosis, treatment and follow-up. Ann Oncol 2018;29:vi19–29.
[2] Weber DC, Peguret N, Dipasquale G, Cozzi L. Involved-node and involved-field volumetric modulated arc vs. fixed beam intensity modulated radiotherapy for female patients with early-stage supradiaphragmatic Hodgkin Lymphoma: a comparative planning study. Int J Radiat Oncol Biol Phys 2009;75:1578–86.
[3] Voong KR, McSpadden K, Pinnix CC, Shihadeh F, Reed V, Salehpour MR, et al. Dosimetric advantages of a "butterfly" technique for intensity-modulated radiation therapy for young female patients with mediastinal Hodgkin's lymphoma. Radiat Oncol 2014;9:94.
[4] Lohr F, Georg D, Cozzi L, Eich HT, Weber DC, Koeck J, et al. Novel radiotherapy techniques for involved-field and involved-node treatment of mediastinal Hodgkin lymphoma: when should they be considered and which questions remain open? Strahlenther Onkol 2014;190:864–6.
[5] Hall EJ, Wuu CS. Radiation-induced second cancers: the impact of 3D-CRT and IMRT. Int J Radiat Oncol Biol Phys 2003;56:83–8.
[6] Ng AK, Bernardo MV, Weller E, Backstrand K, Silver B, Marcus KC, et al. Second malignancy after Hodgkin disease treated with radiation therapy with or without chemotherapy: long term risks and risk factors. Blood 2002;100:1989–96.
[7] Filippi AR, Ragona R, Fusella M, Botticella A, Fiandra C, Ricardi U. Changes in breast cancer risk associated with different volumes, doses, and techniques in female Hodgkin lymphoma patients treated with supra-diaphragmatic radiation therapy. Pract Radiat Oncol 2013;3:216–22.
[8] Filippi AR, Ragona R, Piva C, Scafa D, Fiandra C, Fusella M, et al. Optimized volumetric modulated arc therapy versus 3D-CRT for early stage mediastinal Hodgkin lymphoma without axillary involvement: a comparison of second cancers and heart disease risk. Int J Radiat Oncol Biol Phys 2015;92:161–8.
[9] Weber DC, Johanson S, Peguret N, Cozzi L, Olsen DR. Predicted risk of radiation induced cancers after involved field and involved node radiotherapy with or without intensity modulation for early-stage Hodgkin lymphoma in female patients. Int J Radiat Oncol Biol Phys 2011;81:490–7.
[10] Maraldo MV, Brodin NP, Aznar MC, Vogelius IR, Munck af Rosenschold P, Petersen PM, et al. Estimated risk of cardiovascular disease and second cancers with modern highly conformal radiotherapy for early stage mediastinal Hodgkin lymphoma. Ann Oncol 2013;24:2113–8.
[11] Aznar MC, Maraldo MV, Schut DA, Lundemann M, Brodin NP, Vogelius IR, et al. Minimizing late effects for patients with mediastinal Hodgkin lymphoma: deep inspiration breath-hold, IMRT, or both? Int J Radiat Oncol Biol Phys 2015;92:169–74.
[12] Filippi AR, Vanoni V, Meduri B, Cozzi L, Scorsetti M, Ricardi U, et al. Intensity modulated radiation therapy and second cancer risk in adults. Int J Radiat Oncol Biol Phys 2018;100:17–20.
[13] Fiandra C, Filippi AR, Catuzzo P, Botticella A, Ciammella P, Franco P, et al. Different IMRT solutions vs 3D-conformal radiotherapy in early stage Hodgkin lymphoma: dosimetric comparison and clinical considerations. Radiat Oncol 2012;7:186.
[14] Hancock SL, Tucker MA, Hoppe RT. Factors affecting late mortality from heart disease after treatment of Hodgkin's disease. JAMA 1993;270(16):1949–55.
[15] Aleman BM, van den Belt-Dusebout AW, De Bruin ML, van't Veer MB, Baaijens MH, de Boer JP, et al. Late cardiotoxicity after treatment for Hodgkin lymphoma. Blood 2007;109(5):1878–86.
[16] Galper SL, Yu JB, Mauch PM, Strasser JF, Silver B, Lacasce A, et al. Clinically significant cardiac disease in patients with Hodgkin lymphoma treated with mediastinal irradiation. Blood 2011;117(2):412–8.
[17] van Nimwegen FA, Schaapveld M, Cutter DJ, Janus CP, Krol AD, Hauptmann M, et al. Radiation dose-response relationship for risk of coronary heart disease in survivors of Hodgkin lymphoma. J Clin Oncol 2016;34(3):235–43.
[18] Moignier A, Broggio D, Derreumaux S, Beaudrè A, Girinsky T, Paul JF, et al. Coronary stenosis risk analysis following Hodgkin lymphoma radiotherapy: a study based on patient specific artery segments dose calculation. Radiother Oncol 2015;117:467–72.
[19] Cutter DJ, Schaapveld M, Darby SC, Hauptmann M, van nimwegen FA, Krol AD, et al. Risk for valvular heart disease after treatment for Hodgkin lymphoma. J Natl Cancer Inst 2015;107:008.
[20] Feng M, Moran JM, Koelling T, Chughtai A, Chan JL, Freedman L, et al. Development and validation of a heart atlas to study cardiac exposure to radiation following treatment for breast cancer. Int J Radiat Oncol Biol Phys 2011;79:10–8.
[21] Levis M, De Luca V, Fiandra C, Veglia S, Fava A, Gatti M, et al. Plan optimization for mediastinal radiotherapy: estimation of coronary arteries motion with ECG-gated cardiac imaging and creation of compensatory expansion margins. Radioth Oncol 2018;127:481–6.
[22] Filippi AR, Ciammella P, Piva C, Ragona R, Botto B, Gavarotti P, et al. Involved-site image-guided intensity-modulated radiotherapy vs 3D conformal radiotherapy in supra-diaphragmatic early stage Hodgkin lymphoma. Int J Radiat Oncol Biol Phys 2014;89:370.
[23] Mulrooney DA, Nunnery SE, Armstrong GT, Ness KK, Srivastava D, Donovan FD, et al. Coronary artery disease detected by coronary computed tomography angiography in adult survivors of childhood Hodgkin lymphoma. Cancer 2014;120:3536–44.
[24] Schneider U, Zwahlen D, Ross D, Kaser-Hotz B. Estimation of radiation-induced cancer from three-dimensional dose distributions: concept of organ equivalent dose. Int J Radiat Oncol Biol Phys 2005;61:1510–5.
[25] Schneider U, Sumila M, Robotka J, Weber D, Gruber G. Radiation-induced second malignancies after involved-node radiotherapy with deep-insipiration breath-hold technique for early stage Hodgkin lymphoma: a dosimetric study. Radiat Oncol 2014;9:58.
[26] Kellerer AM, Nekolla EA, Walsh L. On the conversion of solid cancer excess relative risk into lifetime attributable risk. Radiat Environ Biophys 2001;40:249–57.
[27] Darby SC, Ewertz M, McGale P, Bennet AM, Blom-Goldman U, Brønnum D, et al. Risk of ischemic heart disease in women after radiotherapy for breast cancer. N Engl J Med 2013;368:987–98.
[28] van Nimwegen FA, Ntentas G, Darby SC, Schaapveld M, Hauptmann M, Lugtenburg PJ, et al. Risk of heart failure in survivors of Hodgkin lymphoma: effects of cardiac exposure to radiation and anthracyclines. Blood 2018;129(16):2257–65.

[29] Maraldo MV, Giusti F, Vogelius IR, Lundemann M, van der Kaaij MA, Ramadan S, et al. Cardiovascular disease after treatment for Hodgkin's lymphoma: an analysis of nine collaborative EORTC-LYSA trials. Lancet Hematol 2015;2:492–502.
[30] Hahn E, Jiang H, Ng A, Bashir S, Ahmed S, Tsang R, et al. Late cardiac toxicity after mediastinal radiation therapy for Hodgkin lymphoma: contributions of coronary artery and whole heart dose-volume variables to risk prediction. Int J Radiat Oncol Biol Phys 2017;98:1116–23.
[31] Nilsson G, Witt Nystrom P, Isacsson U, Garmo H, Duvernoy O, Sjogren I, et al. Radiation dose distribution in coronary arteries in breast cancer radiotherapy. Acta Oncol 2016;55:959–63.
[32] Berrington de Gonzalez A, Gilbert E, Curtis R, Inskip P, Kleinerman R, Morton L, et al. solid cancers after radiation therapy: a systematic review of the epidemiologic studies of the radiation dose-response relationship. Int J Radiat Oncol Biol Phys 2013;86:224–33.